Organic LETTERS

Letter

pubs.acs.org/OrgLett

Foxo3a Inhibitors of Microbial Origin, JBIR-141 and JBIR-142

Teppei Kawahara,[†] Noritaka Kagaya,[‡] Yuichi Masuda,[§] Takayuki Doi,[§] Miho Izumikawa,[†] Kumiko Ohta,[⊥] Atsushi Hirao,[⊥] and Kazuo Shin-ya*[,‡]

[†]Japan Biological Informatics Consortium (JBIC), 2-4-7 Aomi, Koto-ku, Tokyo 135-0064, Japan

[‡]National Institute of Advanced Industrial Science and Technology (AIST), 2-4-7 Aomi, Koto-ku, Tokyo 135-0064, Japan

[§]Graduate School of Pharmaceutical Sciences, Tohoku University, 6-3 Aza-Aoba, Aramaki, Aoba-ku, Sendai, Miyagi 980-8578, Japan

[⊥]Division of Molecular Genetics, Cancer and Stem Cell Research Program, Cancer Research Institute, Kanazawa University, Kakuma-machi, Kanazawa, Ishikawa 920-1192, Japan

Supporting Information

ABSTRACT: JBIR-141 (**1**) and JBIR-142 (**2**) were discovered as potent Foxo3a inhibitors that consist of three quite unique substructures, a 1-((dimethylamino)ethyl)-5-methyl-4,5-dihydrooxazole-4-carboxylic acid that is originated from Ala-Thr amino acid residues, a 3-acetoxy-4-amino-7-(hydroxy(nitroso)-amino)-2,2-dimethylheptanoic acid, and an α-acyl tetramic acid fused with a 2-methylpropan-1-ol moiety. Their structures involving absolute configurations were determined by spectroscopic data, chemical degradation, anisotropy methods, and LC−MS analyses of diastereomeric derivatives. Compounds **1** and **2** exhibited specific inhibition against Foxo3a transcriptional activity with IC_{50} values of 23.1 and 166.2 nM, respectively.

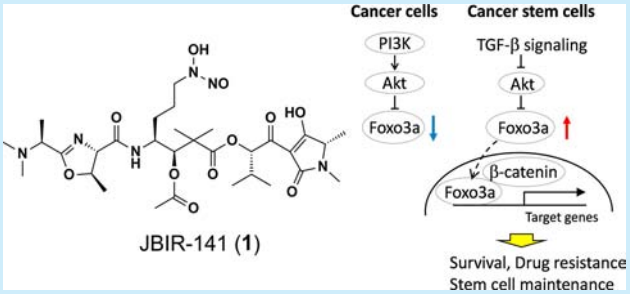

The Foxo3a transcription factor belongs to the forkhead family of class O (Foxo) that plays an important role in energy metabolism, cell cycle arrest, apoptosis, antioxidation, and DNA repair by regulating target genes[1−4] or direct protein−protein interactions.[5] Although development of BCR−ABL tyrosine kinase inhibitors has significantly improved the therapy of chronic myeloid leukemia (CML), it is not absolutely conquered because a small population of cancer stem cells gives rise to drug resistance and CML recurrence.[6] Recent studies proved that Foxo3a is critical for the survival and self-renewal of hematopoietic stem cells[7] and leukemia stem cells.[8,9] In CML model mice, imatinib administration combined with Foxo3a ablation successfully reduced leukemia-initiating cells (LICs). In LICs, PI3K-Akt signaling, an upstream negative regulator of Foxo3a, is suppressed by TGF-β signaling, and activated Foxo3a works for stem cell maintenance in the nucleus.[8] Depletion of Foxo3a could induce maturation of LICs and subsequent cell death.[9] A highly malignant population of cancer stem cells has been reported to contain a large amount of β-catenin in the nucleus, which can change the function of transcription factors by binding to them. A complex of β-catenin and Foxo3a exerts this function on stem cell maintenance without inducing apoptosis.[10] Because difficulties in the treatment of CML with imatinib are brought on by quiescent and undifferentiated cancer stem cells, Foxo3a is expected to be a promising target for eradicating CML stem cells.

During a screening program for Foxo3a inhibitors from our natural product library consisting of over 250000 samples,[11] two potent compounds, JBIR-141 (**1**) and JBIR-142 (**2**) (Figure 1), were isolated from the culture broth of a soil-derived *Streptomyces* sp. 4587H4S (see the Supporting Information). Herein, the isolation, structure determination, and biological evaluation of **1** and **2** are presented.

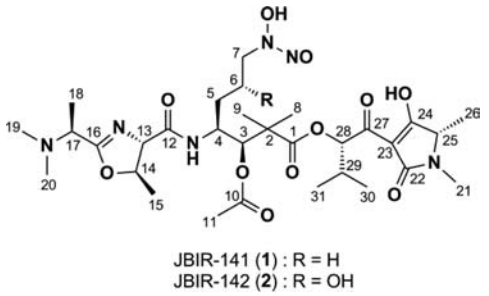

Figure 1. Structures of JBIR-141 (**1**) and JBIR-142 (**2**).

JBIR-141 (**1**) was obtained as a colorless powder, having a molecular formula $C_{31}H_{50}N_6O_{11}$, determined by positive mode HRESIMS at m/z 683.3641 $[M + H]^+$ (calcd for $C_{31}H_{51}N_6O_{11}$, 683.3616). The UV data displayed a peak absorption band at 243 and 288 nm, which suggested the presence of an α-acyl tetramic acid moiety. The IR spectrum exhibited absorption bands for hydroxy (3350 cm^{-1}), ester carbonyl (1733 and 1222 cm^{-1}), amide carbonyl (1616 cm^{-1}), and nitrosohydroxyamino (1457 cm^{-1}) groups.[12−15]

Received: October 1, 2015
Published: October 23, 2015

DOI: 10.1021/acs.orglett.5b02842
Org. Lett. 2015, 17, 5476−5479

The appearance of several amide carbonyl carbon signals in the ^{13}C NMR spectrum intimated the peptide-like nature of the molecule. The planar structure of **1** was mainly elucidated based on the analyses of DQF-COSY and CT-HMBC[16] spectra (Figure 2 and Table S1).

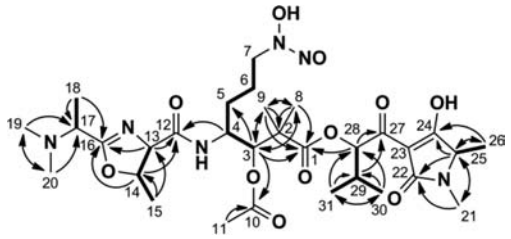

Figure 2. Key correlations in DQF-COSY (bold lines) and CT-HMBC (arrows) spectra of JBIR-141 (**1**).

The ^1H sequence from an oxymethine proton H-3 (δ_H 5.56, δ_C 79.0) through a nitrogen-bonded methine proton H-4 (δ_H 3.93, δ_C 50.9), methylene protons H_2-5 (δ_H 1.77, 1.26), and H_2-6 (δ_H 1.75) to deshielded nitrogen-substituted methylene protons H_2-7 (δ_H 3.95 and 3.90, δ_C 57.5), together with HMBC correlations from singlet methyl protons H_3-8 (δ_H 1.13) and H_3-9 (δ_H 1.03) to an ester carbonyl carbon C-1 (δ_C 172.2), a quaternary carbon C-2 (δ_C 47.2), and an oxymethine carbon C-3 established the presence of a 4,7-diamino-3-hydroxy-2,2-dimethylheptanoic acid moiety. Additional HMBC correlations from H-3 and an acetic methyl proton H_3-11 (δ_H 2.14) to a carbonyl carbon C-10 (δ_C 172.2) indicate that an acetoxy group is located at C-3.

Methyl protons H_3-30 (δ_H 1.05) and H_3-31 (δ_H 1.06) were $^1H-^{13}C$ long-range coupled to each other and commonly coupled to a methine carbon C-29 (δ_C 33.1) and an oxymethine carbon C-28 (δ_C 80.5). Additional $^1H-^{13}C$ long-range couplings from an oxymethine proton H-28 (δ_H 6.15) and a methine proton H-29 (δ_H 2.18) to an α,β-unsaturated carbonyl carbon C-27 (δ_C 192.6) and from H-28 to the ester carbonyl carbon C-1 proved that a 2-hydroxy-3-methylbutanoic acid (valinic acid) residue is substituted at the position of C-1 through an ester bond.

The ^1H sequence from an α-methine proton H-13 (δ_H 3.68, δ_C 75.0) to methyl protons H_3-15 (δ_H 1.11) through an oxymethine proton H-14 (δ_H 4.90) and HMBC correlations between H-13 and an amide carbonyl carbon C-12 (δ_C 172.2) predicted the presence of a threonine-like moiety. $^1H-^{13}C$ long-range couplings from H-13 and H-14 to highly low-field shifted quaternary carbon C-16 (δ_C 172.4) indicated a methyloxazoline residue, which was confirmed by acid hydrolysis vide infra.

HMBC couplings from methyl protons H_3-18 (δ_H 1.34) to a nitrogen-bonded methine carbon C-17 (δ_C 59.8) and C-16 and nitrogen-substituted *gem*-dimethyl protons H_3-19 (δ_H 2.34) and H_3-20 (δ_H 2.34) to the methine carbon C-17 established that a dimethylamino ethane moiety is substituted at the C-16 position. HMBC correlations from the methine proton H-4 to C-12 proved that a 1-((dimethylamino)ethyl)-5-methyl-4,5-dihydrooxazole-4-carboxylic acid substructure is substituted at C-4 through amide bond.

$^1H-^{13}C$ long-range couplings from H_3-26 (δ_H 1.25) to an oxygenated sp^2 carbon C-24 and a nitrogen-bearing methine carbon C-25 (δ_C 62.4) and from an *N*-methyl proton H_3-21 (δ_H 2.91, δ_C 26.6) to an amide carbonyl carbon C-22 (δ_C 173.9) and C-25 were observed. In addition to these HMBC correlations, the characteristic ^{13}C chemical shifts of δ_C 190.1, 194.9, 174.2, and 99.9, along with a characteristic UV absorption for tetramic acid chromophore (UV 288 nm), suggested that an α-acyl 1,5-dimethyltetramic acid moiety[17,18] was connected to the valinic acid moiety.

The remaining one nitrogen and two oxygen atoms, calculated from the molecular formula, were allowed to be a nitrosohydroxyamino group at C-7 because of the specific IR absorption (1457 cm^{-1}). Hence, the planar structure of **1** was determined as shown in Figure 1.

The molecular formula of JBIR-142 (**2**) was determined as $C_{31}H_{50}N_6O_{12}$ on the basis of HRESI(+)MS, suggestive of an oxygenated derivative of **1**. This difference was assigned as 6-OH in **2** by the analyses of 1D and 2D NMR spectra (Figure S2 and Table S1), in which a diagnostic signal (δ_H 4.26, δ_C 67.0) for an oxymethine was observed. Therefore, the planar structure of **2** was determined being a 6-hydroxy **1**.

Since **2** possesses an additional chiral center to **1**, **2** was employed for the determination of the absolute configuration. The desired chemical degradation protocol for the tetramic acid moiety was previously reported.[17,18] According to the protocol, compound **2** was treated with sodium periodate followed by acid hydrolysis to afford an *N*-methylalanine residue. The absolute structure of the obtained *N*-methylalanine was determined to be *S* by the advanced Marfey's method[19,20] (For detailed procedures, see the Supporting Information). Consequently, the absolute configuration at C-25 was established as *S*.

As a congener of **2**, inactive compound **3** (there were no inhibitory activities at the concentration of 5 μM, Figure 6) was isolated together with **1** and **2** (detailed isolation and structure determination of **3** are described in the Supporting Information). Since **3** was considered to be a good compound for the establishment of the absolute configuration of a series of these compounds, chemical degradation was performed on **3** (Scheme 1). To determine the absolute configuration of the remaining chiral centers, compounds **4** and **5** (partial racemic form) were obtained by alkaline hydrolysis of **3** followed by chromatographic

Scheme 1. Procedures for the Degradation of 3

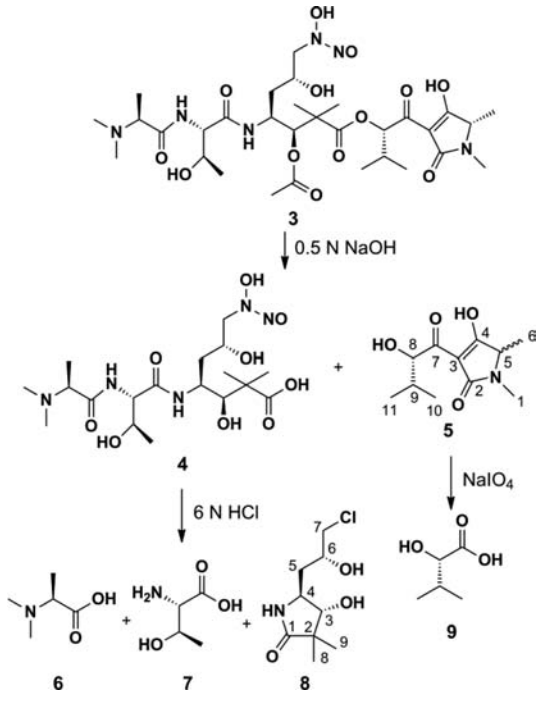

DOI: 10.1021/acs.orglett.5b02842
Org. Lett. 2015, 17, 5476−5479

purification. For planar structure elucidation of **5**, see the Supporting Information.

Compound **4** was acid hydrolyzed (6 N HCl, 110 °C, 16 h), and the solution was dried with blown air. For the assignment of the stereochemistry at C-17, a chromatographic analysis determination using phenylglycine methyl ester (PGME) derivatives was applied.[21,22] The hydrolysate was reacted with (*S*)- or (*R*)-PGME, and the amide products were analyzed by RP-HPLC−MS. The retention times of (*S*)- and (*R*)-PGME derivatives (t_R 7.4 and 8.0 min, respectively) were matched with those of corresponding (*S*)- and (*R*)-PGME derivatives of synthetic *N*,*N*-dimethyl-L-alanine standards, indicating that **6** is in the L-form. Thus, the absolute configuration of C-17 was established as *S*.

The absolute configuration of C-13 and C-14 in the threonine residue were determined as 13*S* and 14*R* by LC−MS analyses in the acid hydrolysate of **4** compared with those of the threonine standard derivatives (advanced Marfey's method, see the Supporting Information).[19]

To obtain **8** as a main component except for amino acid residues, the acid hydrolysate (6 N HCl, 110 °C, 16 h) of **4** was purified by RP-HPLC preparation. The molecular formula of **8** was revealed as $C_9H_{16}ClNO_3$ by HRESIMS. The nitrosohydroxyamino functional group was converted into a chlorine atom whose existence was further supported by the intensity of the isotope peaks' ratio (3:1). The planar structure of **8** was established by the analysis of DQF-COSY and CT-HMBC spectra. COSY correlations from an oxymethine proton H-3 ($\delta_{H/C}$ 3.63/82.6) to chlorinated methylene protons H_2-7 ($\delta_{H/C}$ 3.56, 3.53/50.0) through nitrogen-substituted methine proton H-4 ($\delta_{H/C}$ 3.42/57.9), aliphatic methylene protons H_2-5 ($\delta_{H/C}$ 2.06, 1.59/38.9), and an oxymethine proton H-6 ($\delta_{H/C}$ 3.99/71.7) and HMBC correlations from *gem*-methyl protons H_3-8 and H_3-9 ($\delta_{H/C}$ 1.14/22.9 and 1.05/18.1, respectively) to an oxymethine carbon C-3, a quaternary carbon C-2, and a carbonyl carbon C-1 (δ_C 182.5) were observed. The relatively low field shifted ^{13}C chemical shift value against ordinal lactone or lactam functions along with the lack of low field shifted (acylated shift) ^1H chemical shift values at C-3 and C-6 in **8** were suitable to judge the presence of a γ-lactam ring (Figure S4 and Table S2). Thus, the planar structure of **8** was established to be a 5-(3-chloro-2-hydroxypropyl)-4-hydroxy-3,3-dimethyl-2-pyrrolidinone.

The relative configuration of the C-3/C-4 axis in **8** was determined by NOESY (Figure 3). Strong NOESY correlations of H-3/H_3-8 and H-4/H_3-9 were observed, whereas the correlation of H-3/H_3-9 was observed weakly, which was indicative that H-4 is located on the same side as C-9 and the opposite side of H-3 and C-8 on the γ-lactam ring. Thus, the relative configurations of C-3 and C-4 were deduced as 3*R** and 4*S**. The relative configuration of C-4/C-5/C-6 was established

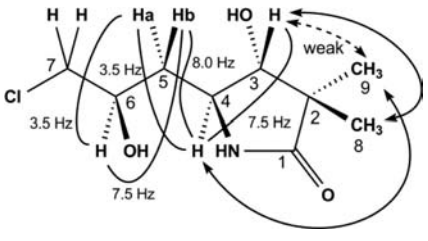

Figure 3. Key NOESY correlations (arrow) and $^1H-^1H$ coupling constants of **8**.

by the *J*-based configuration analysis using vicinal $^1H-^1H$ and long-range $^1H-^{13}C$ coupling constants.[23,24] At the C-4/C-5 axis, a large coupling constant between H-4 and Hb-5 (8.0 Hz) indicated the anti orientation of H-4/Hb-5. A small $^3J_{H-C}$ coupling constant ($^3J_{Ha\text{-}5\text{-}C\text{-}3}$ < 3 Hz) obtained from the *J*-resolved HMBC-2[25] spectrum showed Ha-5 and C-3 are in the gauche orientation. These results revealed that C-3/C-6 and 4-N/Ha-5 are in anti orientations, as shown in Figure 4. For the C-

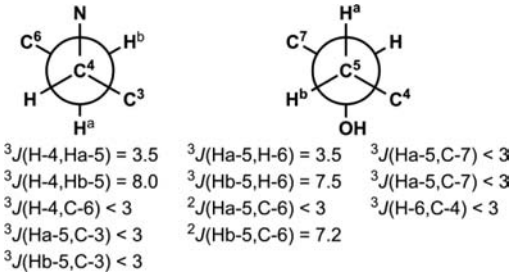

Figure 4. *J*-based configuration analysis of **8**.

5/C-6 axis, the large $^1H-^1H$ coupling constant (7.5 Hz) between Hb-5 and H-6 and a small $^2J_{C-H}$ coupling constant (<3 Hz) between Ha-5 and C-6 inferred that C-4/C-7 and Ha-5/6-O are in anti orientations. Given these information, the relative configuration of **8** was deduced as 3*R**, 4*S**, 6*R**.

Determination of the absolute configuration was attempted by derivatizing **8** with (*R*)- and (*S*)-α-methoxy-α-(trifluoromethyl)-phenylacetyl (MTPA) chloride and applying for the modified Mosher's method. Compound **8** was treated with (*R*)- and (*S*)-MTPACl in pyridine to give (*S*)- and (*R*)-MTPA diester derivatives, respectively. The stereochemical determination was based on the chemical shift differences of the protons as shown in Figure 5. The $\Delta\delta$ values ($\delta_S - \delta_R$) of the methyl protons of C-2

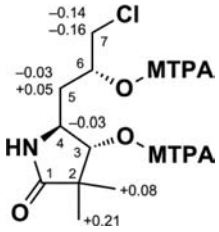

Figure 5. $\Delta\delta$ values [$\Delta\delta$ (in ppm) = $\delta_S - \delta_R$] obtained for the (*S*)- and (*R*)-MTPA diesters of **8**.

(+0.08, + 0.21) showed positive, while those of H-4 (−0.03) and one of H_2-5 (−0.03) were negative, thus suggesting the 3*R*-configuration. The positive $\Delta\delta$ value of one of H_2-5 (+0.05) and negative $\Delta\delta$ values of H_2-7 (−0.14, −0.16) were interpreted as the 6*R* configuration. Thus, the absolute configuration of **8** was consequently assigned to be 3*R*,4*S*,6*R*.

Compound **5** was degradated by sodium periodate to yield 2-hydroxy-3-methylbutanoic acid (valinic acid, **9**), whose absolute configuration was determined to be *S* by the chromatographic analyses of the PGME derivatives (see the Supporting Information). The retention times of (*R*)- and (*S*)-PGME derivatives of **9** (t_R 13.8 and 14.2 min, respectively) were matched with those of (*R*)- and (*S*)-PGME derivatives of authentic (*S*)-2-hydroxy-3-methylbutanoic acid. Therefore, the absolute configuration of C-8 of **5** was established to be *S*. Hence, the absolute configurations of a series of unique novel compounds in this study were defined as shown in Figure 1.

DOI: 10.1021/acs.orglett.5b02842
Org. Lett. 2015, 17, 5476−5479

Compounds **1** and **2** exhibited exceptionally potent specific inhibition against Foxo3a transcriptional activity in a cell-based reporter assay, while compound **3** possessed no detectable activity. The results are summarized in Figure 6, and IC_{50} values

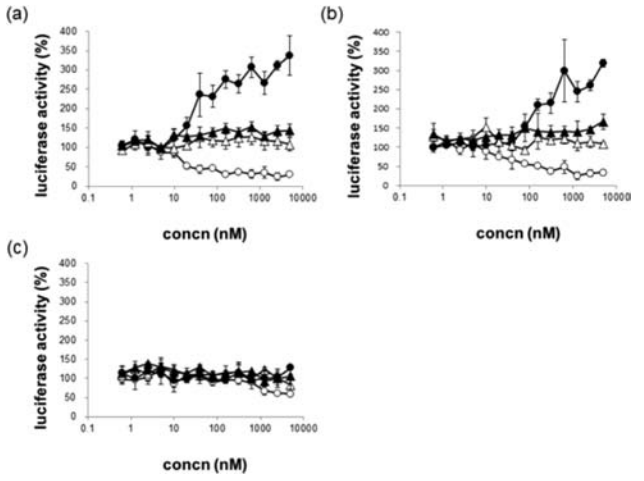

Figure 6. Specific Inhibition of Foxo3a transcriptional activity by (a) JBIR-141 (**1**), (b) JBIR-142 (**2**), and (c) **3**: (○) Foxo3a, (●) NF-kB, (Δ) p53, (▲) notch.

of **1** and **2** are 23.1 and 166.2 nM, respectively. As observed in Figure 6, **1** and **2** showed good selectivity against Foxo3a compared with other transcription factors NF-κB, p53, and notch. Interestingly, **1** and **2** up-regulated NF-κB transcriptional activity in contrast to Foxo3a. Cell viabilities almost did not changed during 24 h treatment with compounds (data not shown).

Cytotoxic activities were also evaluated using human ovarian adenocarcinoma SKOV-3, human malignant mesothelioma MESO-1, and human T-lymphoma Jurkat cell lines after 72 h treatment with compounds. IC_{50} values of compounds **1**, **2**, and **3** were 11.7, 101, and 1094 nM in SKOV-3 cells, 89.8, 66.5, and 3353 nM in MESO-1 cells, and 4.41, 30.6, and 836 nM in Jurkat cells, respectively. As listed above, **1** and **2** showed strong anticancer activities.

Examination of their detailed biological activities and determination of the target molecule of these compounds by chemical biology strategies are now underway.

■ ASSOCIATED CONTENT

Supporting Information

The Supporting Information is available free of charge on the ACS Publications website at DOI: 10.1021/acs.orglett.5b02842.

Experimental details and characterization data (PDF)

■ AUTHOR INFORMATION

Corresponding Author

*E-mail: k-shinya@aist.go.jp.

Notes

The authors declare no competing financial interest.

■ ACKNOWLEDGMENTS

This work was supported in part by a grant "Project focused on developing key technologies for discovering and manufacturing drugs for next-generation treatment and diagnosis" from the Ministry of Economy, Trade and Industry (METI) and in part by a grant "Project for Development of Innovative Research on Cancer Therapeutics (P-DIRECT)" from the Ministry of Education, Culture, Sports, Science and Technology (MEXT).

■ REFERENCES

(1) Eijkelenboom, A.; Burgering, B. M. T. *Nat. Rev. Mol. Cell Biol.* **2013**, *14*, 83−97.
(2) Morris, B. J.; Willcox, D. C.; Donlon, T. a.; Willcox, B. J. *Gerontology* **2015**, 515.
(3) Essafi, A.; Fernández de Mattos, S.; Hassen, Y. a M.; Soeiro, I.; Mufti, G. J.; Thomas, N. S. B.; Medema, R. H.; Lam, E. W.-F. *Oncogene* **2005**, *24*, 2317−2329.
(4) Fu, Z.; Tindall, D. J. *Oncogene* **2008**, *27*, 2312−2319.
(5) Daitoku, H.; Sakamaki, J. I.; Fukamizu, A. *Biochim. Biophys. Acta, Mol. Cell Res.* **2011**, *1813*, 1954−1960.
(6) Naka, K.; Hoshii, T.; Hirao, A. *Cancer Sci.* **2010**, *101*, 1577−1581.
(7) Miyamoto, K.; Araki, K. Y.; Naka, K.; Arai, F.; Takubo, K.; Yamazaki, S.; Matsuoka, S.; Miyamoto, T.; Ito, K.; Ohmura, M.; Chen, C.; Hosokawa, K.; Nakauchi, H.; Nakayama, K.; Nakayama, K. I.; Harada, M.; Motoyama, N.; Suda, T.; Hirao, A. *Cell Stem Cell* **2007**, *1*, 101−112.
(8) Naka, K.; Hoshii, T.; Muraguchi, T.; Tadokoro, Y.; Ooshio, T.; Kondo, Y.; Nakao, S.; Motoyama, N.; Hirao, A. *Nature* **2010**, *463*, 676−680.
(9) Sykes, S. M.; Lane, S. W.; Bullinger, L.; Kalaitzidis, D.; Yusuf, R.; Saez, B.; Ferraro, F.; Mercier, F.; Singh, H.; Brumme, K. M.; Acharya, S. S.; Schöll, C.; Tothova, Z.; Attar, E. C.; Fröhling, S.; Depinho, R. A.; Armstrong, S. A.; Gilliland, D. G.; Scadden, D. T. *Cell* **2011**, *146*, 697−708.
(10) Tenbaum, S. P.; Ordóñez-Morán, P.; Puig, I.; Chicote, I.; Arqués, O.; Landolfi, S.; Fernández, Y.; Herance, J. R.; Gispert, J. D.; Mendizabal, L.; Aguilar, S.; Cajal, S. R. Y.; Schwartz, S.; Vivancos, A.; Espín, E.; Rojas, S.; Baselga, J.; Tabernero, J.; Muñoz, A.; Palmer, H. G. *Nat. Med.* **2012**, *18*, 892−901.
(11) Kawahara, T.; Hwang, J.-H.; Izumikawa, M.; Hashimoto, J.; Takagi, M.; Shin-Ya, K. *J. Nat. Prod.* **2012**, *75*, 1814−1818.
(12) Nishio, M.; Hasegawa, M.; Suzuki, K.; Sawada, Y.; Hook, D. J.; Oki, T. *J. Antibiot.* **1993**, *46*, 193−195.
(13) Fushimi, S.; Nishikawa, S.; Mito, N.; Ikemoto, M.; Sasaki, M.; Seto, H. *J. Antibiot.* **1989**, *42*, 1370−1378.
(14) Strazzolini, P.; Malabarba, A.; Ferrari, P.; Grandi, M.; Cavalleri, B. *J. Med. Chem.* **1984**, *27*, 1295−1299.
(15) Strazzolini, P.; Dall'Arche, M.; Zossi, M.; Pavsler, A. *Eur. J. Org. Chem.* **2004**, 4710−4716.
(16) Furihata, K.; Seto, H. *Tetrahedron Lett.* **1998**, *39*, 7337−7340.
(17) Ikeda, H.; Matsumori, N.; Ono, M.; Suzuki, A.; Isogai, A.; Nagasawa, H.; Sakuda, S. *J. Org. Chem.* **2000**, *65*, 438−444.
(18) Sawa, R.; Takahashi, Y.; Hashizume, H.; Sasaki, K.; Ishizaki, Y.; Umekita, M.; Hatano, M.; Abe, H.; Watanabe, T.; Kinoshita, N.; Homma, Y.; Hayashi, C.; Inoue, K.; Ohba, S.; Masuda, T.; Arakawa, M.; Kobayashi, Y.; Hamada, M.; Igarashi, M.; Adachi, H.; Nishimura, Y.; Akamatsu, Y. *Chem. - Eur. J.* **2012**, *18*, 15772−15781.
(19) Marfey, P. *Carlsberg Res. Commun.* **1984**, *49*, 591−596.
(20) Fu, P.; Jamison, M.; La, S.; MacMillan, J. B. *Org. Lett.* **2014**, *16*, 5656−5659.
(21) Nagai, Y.; Kusumi, T. *Tetrahedron Lett.* **1995**, *36*, 1853−1856.
(22) Um, S.; Choi, T. J.; Kim, H.; Kim, B. Y.; Kim, S.-H.; Lee, S. K.; Oh, K.-B.; Shin, J.; Oh, D.-C. *J. Org. Chem.* **2013**, *78*, 12321−12329.
(23) Matsumori, N.; Kaneno, D.; Murata, M.; Nakamura, H.; Tachibana, K. *J. Org. Chem.* **1999**, *64*, 866−876.
(24) Kawahara, T.; Izumikawa, M.; Takagi, M.; Shin-Ya, K. *Org. Lett.* **2012**, *14*, 4434−4437.
(25) Furihata, K.; Seto, H. *Tetrahedron Lett.* **1999**, *40*, 6271−6275.

DOI: 10.1021/acs.orglett.5b02842
Org. Lett. 2015, 17, 5476−5479